Heliyon 10 (2024) e39777

Contents lists available at ScienceDirect

Heliyon

journal homepage: www.cell.com/heliyon

Research article

Functional characterization and unraveling the structural determinants of novel steroid hydroxylase CYP154C7 from *Streptomyces* sp. PAMC26508

Prakash Paudel [a,1], Kamal Prasad Regmi [a,1], Ki-Hwa Kim [b], Jun Hyuck Lee [c], Tae-Jin Oh [a,b,d,*]

[a] Department of Life Science and Biochemical Engineering, Graduate School, Sunmoon University, Asan, 31460, Republic of Korea
[b] Genome-based BioIT Convergence Institute, Asan, 31460, Republic of Korea
[c] Research Unit of Cryogenic Novel Materials, Korea Polar Research Institute, Incheon, 21990, Republic of Korea
[d] Department of Pharmaceutical Engineering and Biotechnology, Sunmoon University, Asan, 31460, Republic of Korea

ARTICLE INFO

Keywords:
Steroid hydroxylases
Cytochrome P450
Streptomyces
Molecular docking
Biocatalyst

ABSTRACT

This study characterized cytochrome P450 enzyme CYP154C7 from *Streptomyces* sp. PAMC26508, emphasizing its capability to hydroxylate steroids, especially at the 16α-position. The enzymatic assay of CYP154C7 demonstrated effective conversion across a pH range of 7.2–7.6, with optimal activity at 30 °C in the Pdx/PdR plus NADH system. Kinetic analysis on most converted steroids (androstenedione and adrenosterone) was performed which shows a greater affinity for androstenedione (K_m, 11.06 ± 1.903 μM; V_{max}, 0.0062 ± 0.0002 sec^{-1}) compared to adrenosterone (K_m, 34.50 ± 6.2 μM; V_{max}, 0.0119 ± 0.0007 sec^{-1}). A whole-cell system in *Escherichia coli*, overexpressing recombinant CYP154C7, achieved substantial conversion for steroids, indicating that CYP154C7 can also be used as a potential whole-cell biocatalyst. To gain structural insights, homology models of CYP154C7 and its homologs were constructed using CYP154C5 (PDB ID: 6TO2), refined, validated, and used for docking studies. Comparative docking analysis suggests that lysine (K236) in the active site and tyrosine (Y197) in the substrate access channel of CYP154C7 are crucial for substrate selectivity and catalytic efficiency. This study suggests that CYP154C7 could be a promising candidate for developing modified steroids, providing valuable insights for protein engineering to design commercially useful CYP steroid hydroxylases with diverse substrate specificities.

1. Introduction

Steroids are a family of terpenoid lipids widely distributed in nature and originate from cholesterol. The process of steroid biosynthesis commences as cholesterol converts into pregnenolone via the action of the cholesterol side chain cleavage enzyme [1]. In pharmaceuticals, steroids hold a significant global market share and are produced in large quantities annually [2]. Steroid-based drugs have been utilized for various health conditions such as arthritis, autoimmune diseases, inflammation, cancer, osteoporosis, HIV, and

* Corresponding author. Department of Life Science and Biochemical Engineering, Graduate School, Sunmoon University, Asan, 31460, Republic of Korea.
E-mail address: tjoh3782@sunmoon.ac.kr (T.-J. Oh).
[1] Prakash Paudel and Kamal Prasad Regmi contributed equally to this work.

https://doi.org/10.1016/j.heliyon.2024.e39777
Received 30 July 2024; Received in revised form 23 October 2024; Accepted 23 October 2024
Available online 24 October 2024

COVID-19, etc. [3–9]. The precise and selective introduction of different functional groups to the steroid structure is crucial for achieving the desired physiological and medicinal effects of steroidal drugs, such as hydroxyl groups at various positions and configurations frequently imparting distinct pharmacological properties [10,11]. For instance, 6β-hydroxyprogesterone is linked to breast cancer inhibitors, while 9α-hydroxyprogesterone is involved in synthesizing substances with glucocorticoid and progestational activity. Additionally, 11α-hydroxyprogesterone regulates blood pressure, serves as a precursor for cortisone and hydrocortisone, and shows potential for treating male hair loss [12,13]. Similarly, hydroxylated forms of dehydroepiandrosterone and epiandrosterone at the 7 positions have neuroprotective effects, cardioactive steroids typically possess a 14β-hydroxyl group, 15α-hydroxylated steroids play a crucial role as intermediates in the synthesis of contraceptives, and the 16α-hydroxyl function plays a critical role in synthetic glucocorticoids like triamcinolone and dexamethasone [14–19]. The cytochrome P450 (CYP)-mediated hydroxylation of steroids stands as a pivotal method for their modification and subsequent functional diversification [20].

The CYPs superfamily comprises a diverse group of heme-containing enzymes, present in all life forms, including plants, animals, fungi, and bacteria (excluding *Escherichia coli* and *Salmonella typhimurium*), and even in some non-living entities such as viruses [21–23]. In nature, CYPs catalyze numerous reactions that are involved in many physiologically important reactions, such as drug metabolism, the biosynthesis of compounds (such as steroids and aromatic compounds), and oxygen-mediated hydroxylation [24]. Bacterial CYP enzymes demonstrate remarkable catalytic activity in hydroxylating inert C-H bonds using molecular oxygen, a feat that is challenging to achieve through chemical means [24–27]. As a result, they are gaining significant interest as potential biocatalysts for chemical transformations.

Among bacterial CYPs, several families have exhibited their remarkable capabilities in steroid hydroxylation. From the CYP102 family, BM3 is recognized as one of the most active and widely studied CYP and is easily expressed at a high level in *E. coli* [28]. Although BM3 typically acts on fatty acids, a series of mutagenesis techniques has expanded its capabilities, making it highly effective in hydroxylating steroids with a wide range of substrates [20,29,30]. Other CYPs including the CYP105 family (CYP105A1, CYP105D5, CYP105D7, and CYP105D18) [31–33], the CYP106 family (CYP106A1, CYP106A2, and CYP106A6) [34,35], the CYP 109 family (CYP109A2, CYP109B1, CYP109E1, and CYP109Q5) [36–39], and the CYP260 family (CYP260A1 and CYP260B1) [40,41] have been characterized and extensively studied for the hydroxylation of steroids. Similarly, from the CYP154 family, CYPs have shown substrate flexibility with different steroids and exhibited interesting product formation patterns. CYP154C5 was the first stereospecific hydroxylase identified in 2006 from this family [33], and subsequently, other related members including CYP154C2, CYP154C3, CYP154C4_1, CYP154C4_2, and CYP154C8 [42–45], were discovered for steroid hydroxylation. Recently, we have reported that two more CYPs from the CYP154 family, CYP154C3_1 and CYP154C3_2, from *Streptomyces* sp. are potential candidates for steroid hydroxylation [46]. Furthermore, in this research, we have introduced another new member from the CYP154 family for steroid hydroxylation, namely CYP154C7. CYP154C7 exhibits the highest degree of similarity to CYP154C8, CYP154C5, CYP154C3_1, and CYP154C3_2, suggesting a strong likelihood of catalytic resemblance among these enzymes. However, despite these enzymes sharing significant similarities, their rates of steroid hydroxylation conversion and substrate flexibility vary. Additionally, there is currently no available 3D structural data or molecular-level explanation for CYP154C8, CYP154C3_1, and CYP154C3_2. Thus, this lack of structural data and explanation of enzyme-substrate interaction hinders gaining valuable insights for further protein engineering and designing applicable CYP steroid hydroxylases with different substrate specificities.

Here, inspired by the previous study, we have characterized a previously unrecognized steroid-hydroxylating enzyme belonging to the CYP154 family, CYP154C7, originating from *Streptomyces* sp. PAMC26508. We have extensively investigated its potential for facilitating the hydroxylation of diverse steroid compounds via *in-vitro* reactions, and *in-vivo* reactions. Furthermore, addressing the challenges of lack of 3D structures and explanation of enzyme-substrate interaction, we performed homology modeling, and docking and compared the interaction of CYP154 enzymes (CYP154C7 and their homolog) with selected steroids to understand enzyme-substrate interactions at the molecular level for steroid hydroxylation.

2. Materials and methods

2.1. Chemical reagents

All the steroid substrates of HPLC grade were purchased from TCI (Tokyo Chemical Industry Co, Ltd, Korea). Isopropyl 1-thio-β-D-galactopyranoside (IPTG) and kanamycin were purchased from Duchefa Bohemie (Korea). The 5-aminolaevulinic acid (ALA), ampicillin (Amp), NADH, catalase, sodium formate, and formate dehydrogenase were obtained from Sigma-Aldrich (Korea). Restriction enzymes were purchased from TaKaRa Clontech (Korea). DNA polymerase, T4 DNA ligase, and dNTPs were purchased from Takara Bio (Japan).

2.2. Bioinformatics analysis

Homolog searching for CYP154C7-like proteins was performed by the Basic Local Alignment Search Tool (BLAST) in the National Center for Biotechnology Information (NCBI) server. Multiple sequence alignments and pairwise sequence alignments (with most close homologs) were done with the program search and sequence analysis tools services from EMBL-EBI [47]. Amino acid sequence analysis was performed and graphically represented using ESPript 3.0 server [48]. An evolutionary relationship and patterns of CYP154C7 were inferred by using MEGA X [49]. The phylogenetic tree was built using the maximum likelihood technique (1000 bootstrap repeats, Poisson correction method) [50]. The name, CYP154C7 was assigned by approved CYP nomenclature (David R. Nelson, Univ. of Tennessee) (https://drnelson.uthsc.edu/CytochromeP450.html).

2.3. Molecular cloning, over-expression, and purification of CYP154C7 and redox partner

The CYP154C7 gene (accession No. AGJ58508) was amplified by PCR from the genomic DNA of *Streptomyces* sp. PAMC26508. The amplified gene containing the restriction sites *Eco*RI/*Hin*dIII (introduced by the specific primers through PCR) was cloned in the pMD20-T (Takara, Japan) vector and transformed into *E. coli* XL1-Blue for gene amplification. After the sequence confirmation, the genes were inserted into the pET-32a(+) vector to construct pET-32a(+)_CYP154C7. This construct was transformed into *E. coli* XL1-Blue and, ultimately, into the over-expression host *E. coli* BL21(DE3). The overexpression and purification of CYP154C7 were performed as described in our previous work [46]. The redox partners putidaredoxin reductase (PdR, *camA*) and putidaredoxin (Pdx, *camB*) were also expressed in *E. coli* BL21(DE3) and purified using the same methods as previously outlined [51].

2.4. Characterization of hydroxylation activity of CYP154C7

Firstly, the concentration of CYP154C7 and redox partners (Pdx and PdR) were measured as described previously [43]. Then, we conducted 300 μL reaction volumes using the CYP154C7 protein in 50 mM potassium phosphate buffer (pH 7.4). The reaction mixture comprised of (CYP:PdR:Pdx ratio 1:2:8) CYP154C7 (3 μM), PdR (6 μM), Pdx (24 μM), substrate (200 μM), catalase (100 μg/mL), and an NADH regeneration system comprising formate dehydrogenase (1.0 U), sodium formate (150 mM), and $MgCl_2$ (1.0 mM) in 50 mM potassium phosphate buffer (pH 7.4). Eleven different steroids (Fig. S1), dissolved in DMSO, were employed as substrates for the enzymatic activity assays. The reaction was initiated by adding 300 μM NADH, incubated for 2 h at 30°C with shaking, and quenched by a double volume of chilled ethyl acetate. The ethyl acetate organic layer was collected, evaporated, dissolved in chilled methanol, and analyzed by HPLC and liquid chromatography-mass spectrometry (LC-MS).

2.5. Effect of temperature and pH on enzymatic activity and kinetic evaluation

The optimal hydroxylation activity of CYP154C7 was measured across a pH range of 6.0–8.5 using a 50 mM potassium phosphate buffer. Temperature-dependent activity was assessed at pH 7.4 across 15–50 °C. Androstenedione served as the substrate in a reaction mixture containing enzyme CYP154C7, PdR, Pdx, catalase, and NADH, followed by extraction with ethyl acetate and evaporation for analysis.

Kinetic analyses were performed for the two most converted substrates, androstenedione and adrenosterone. To determine the K_m and V_{max} parameters for hydroxylation of these substrates, the reactions were assayed in a reaction mixture consisting of 1.0 μM CYP154C7, 2.0 μM PdR, 6.0 μM Pdx, and 100 μM substrate, all dissolved in a 50 mM potassium phosphate buffer (pH 7.4). The reaction was initiated by adding 300 μM NADH and was later stopped by adding an equal volume of methanol after 2 h of incubation at 30 °C. Initial velocity and saturation curves were determined under identical reaction conditions, with varying substrate concentrations (0–200 μM). The products were analyzed by HPLC, employing the same methodology described for the bioconversion assay [43]. K_m and V_{max} values for substrates were calculated by plotting the reaction rate versus substrate concentration. The kinetic analysis was performed using non-linear regression based on Michaelis-Menten kinetics, with GraphPad Prism 8.0 software (La Jolla, California, USA).

2.6. Determination of the substrate dissociation constant

We selected three steroids (androstenedione, testosterone, and cortisone) from our substrate list based on their different conversion rates. Experiments were then conducted to investigate substrate binding in CYP154C7, with substrate binding being assayed by following the substrate-induced spin-shift of the enzyme. We performed substrate binding assays as described previously [43]. The samples' absorption spectra were recorded using a Biochrome Libra S35PC UV/Vis spectrophotometer (England). The difference between the peak and trough (ΔAbs) was graphed against the concentration of the substrate and then analyzed using a non-linear tight-binding equation [52]. The dissociation constant (K_D) was subsequently determined using OriginPro software.

2.7. In-silico analysis

For modeling of the CYP154C7 and their homolog (CYP154C3_1, CYP154C3_2, and CYP154C8), the crystal structure of CYP154C5 (PDB ID: 6TO2, close homolog) as a template was chosen. 3D models of all the proteins were generated using a SWISS-MODEL (https://swissmodel.expasy.org/interactive). The homology models were validated by PROCHECK [53], Verify-3D [54], and ERRAT [55]. Docking simulations were performed with AutoDock Vina-1.1.2 to explore the binding interactions between protein and substrates [56]. AutoDock Tools 1.5.6 was utilized to produce the PDBQT files for both the protein and ligand, along with defining the grid box [57]. Visualization of the results was performed using PyMOL [58]. Furthermore, the substrate access tunnels of selected CYPs were compared using the CAVER 3.0 software tool [59].

2.8. Whole-cell biotransformation

The genes PdR and Pdx, previously cloned into the pCDFDuet vector were introduced into *E. coli* cell BL21(DE3) containing the plasmid [pET-32a(+)-CYP154C7] for whole-cell biotransformation [43]. The *E. coli* cells harboring pET-32a (+)-CYP154C7-(pCDFDuet_Pdx/PdR) were cultured at 37°C in an LB medium containing necessary antibiotics. When the OD_{600}

reached 0.6, protein expression was initiated by adding 1.0 mM ALA, 0.5 mM $FeCl_3$, and 0.5 mM IPTG. Then, the culture was left to incubate for 48 h at 20°C. After incubation, the cells were harvested through centrifugation (3500 rpm) for 20 min at 4°C, followed by two washes with 50 mM potassium phosphate buffer (pH 7.4). The cells, resuspended in the same buffer with 1 mg/mL glucose and 0.5 mM substrate, underwent bioconversion (carried out on a 1.0 mL scale for analytical purposes) for 24 h at 30 °C and 200 rpm. The reaction was stopped by adding an equal volume of ethyl acetate, which was dried, and dissolved in chilled methanol. The product analysis was conducted using the same method as that described for the *in-vitro* assays.

2.9. HPLC and LC-MS analysis

The reaction mixture dissolved in methanol was filtered using a 0.2 μm pore polytetrafluorethylene filter which was injected into an ultra-HPLC instrument and separated using a Shim-pack GIS C18 column (250 × 4.6 mm, 5 μm, Kanto Chemical, Japan). At a flow rate of 1 mL/min, 0.1 % TFA (trifluoroacetic acid) containing water (A), and acetonitrile (B) were utilized as the mobile phase in a gradient system of B at 10 % for 0–1 min, 50 % for 1–8 min, 70 % for 8–14 min, 95 % for 14–17.5 min, and 10 % for 17.5–24 min. Each elution was run for 24 min. UV absorbance at 250 nm was used to detect the substrates and their products. The product from androstenedione, progesterone, and testosterone was correlated with the standard retention time in the HPLC chromatogram. For the remaining substrate products, we compared them to previously reported products [43,46,60]. Further, the reaction mixture was analyzed using a SYNAPT G2-S/ACUITY UPLC liquid chromatography quadrupole time-of-flight/electrospray ionization mass spectrometer (Waters, USA), operating in the positive ion mode.

3. Results and discussion

3.1. Bioinformatics analysis

To understand the phylogenetic relationships of CYP154C7 with other known CYP154 enzymes, we constructed a phylogenetic tree using the maximum-likelihood method (Fig. S2). The phylogenetic tree and an amino acid sequence alignment indicated that CYP154C7 is more closely related to the previously studied CYP154C3_1, CYP154C3_2, CYP154C5, and CYP154C8, sharing a sequence identity of approximately 83.4 %, 81.8 %, 64.4 %, and 74.8 %, respectively (Table S1). An amino acid sequence comparison between the CYP154C7 and its closet homologs was performed. The CYP characteristics, including distinctive oxygen-binding and activating motifs such as the I-helix and K helix (EXXR), as well as the heme-binding domain, are conserved in all proteins, along with a crucial acid-alcohol pair, glutamate, and threonine residues which are known to facilitate oxygen activation in CYPs (Fig. S3).

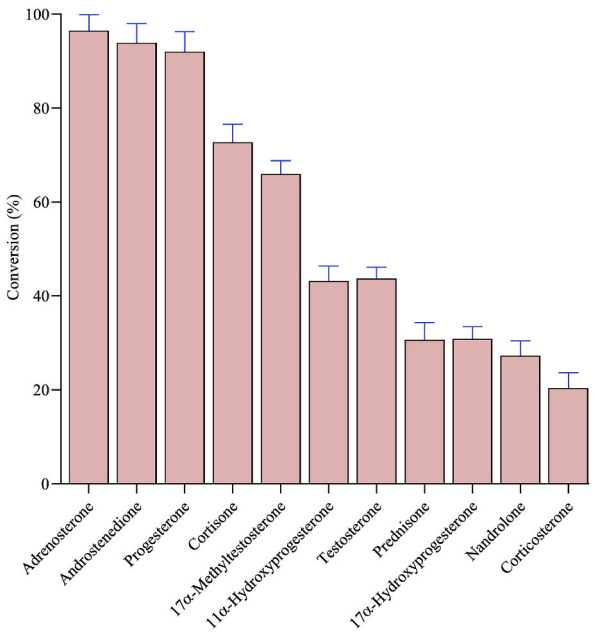

Fig. 1. Product formation in *in-vitro* assays with purified enzyme, CYP154C7. All *in-vitro* reactions were carried out in the presence of 200 μM substrate concentration conducted for 2 h at 30 °C and 1000 rpm. The percentage turnover was determined by calculating the ratio of the product peak area to the sum of the substrate and product area in the HPLC analysis. The mean and standard deviation were calculated based on three independent reactions conducted under similar conditions.

3.2. Expression, purification, and spectral characterization of CYP154C7

CYP154C7 was cloned, overexpressed in E. coli BL21(DE3), and purified, yielding a single homogenous protein band in the soluble fraction on SDS-PAGE (Fig. S4A). The theoretical molecular mass of CYP154C7 was 44.98 kDa, but SDS-PAGE showed a larger band around 65 kDa. This increase was due to the His-Tag/thrombin/T7-Tag sequence in the pET-32a(+) vector, which was fused to CYP154C7's N-terminal region and co-expressed with it. The purified CYP154C7, characterized by a CO-reduction assay, had an Rz value of 1.45, indicating high purity. Its oxidized spectrum showed absorption at 418 nm, typical of CYP enzymes. The carbon monoxide-bound and dithionite-reduced forms displayed maximum absorption at 450 nm, confirming the heme in its native Fe^{2+} CO complex form (Fig. S4B).

3.3. Characterization of hydroxylation activity of CYP154C7

In our preliminary investigation, we identified the redox partner for CYP154C7. Two heterologous redox partners, Pdx/PdR from *P. putida* and Fdx/FdR from spinach, as well as chemical redox partners, hydrogen peroxide and (diacetoxyiodo) benzene, were used in the *in-vitro* reactions. Progesterone, a substrate hydroxylated by previously identified CYP154 family members, was selected to determine the redox partner for bioconversion. When Pdx/PdR served as the redox source, a distinct product peak was observed, while other redox partners showed minimal or no activity. Consequently, PdR/Pdx was selected for the *in-vitro* tests. We carried out an *in-vitro* screening of eleven different steroids (Fig. S1), and the products cast high to low conversion percentages for different substrates (Fig. 1 and Table S2).

Product identification was accomplished by co-eluting reaction mixtures with standard products in HPLC, analyzing retention times, followed by mass data analysis. Furthermore, we compared these results with our previous work. The HPLC chromatograms show that the retention times of the 16α-hydroxyandrostenedione, 16α-hydroxyprogesterone, and 16α-hydroxytestosterone standards have been perfectly aligned with the corresponding products of androstenedione, progesterone, and testosterone, respectively (Fig. 2). LC-MS results show that for the steroid androstenedione, the exact mass of the parent compound was measured as m/z^+ $[M+H]^+$ 287.2005 amu, while the single product had an exact mass of m/z^+ $[M+H]^+$ 303.1963 amu. The calculated mass for the chemical formula $C_{19}H_{27}O_3^+$ is 303.4166 amu (Fig. 2A and Table S3). For the steroid progesterone, the exact mass of the parent compound was m/z^+ $[M+H]^+$ 315.2325 amu, and the single product had an exact mass of m/z^+ $[M+H]^+$ 331.2276 amu. The theoretical formula mass

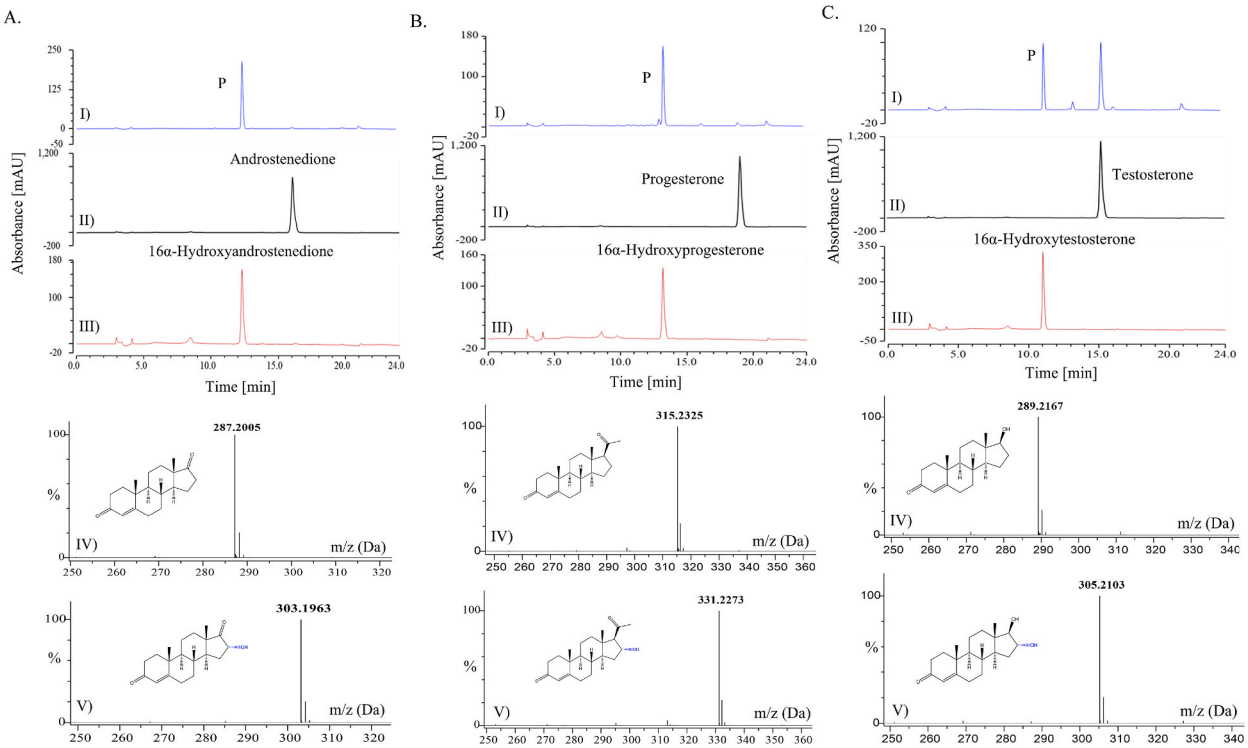

Fig. 2. HPLC chromatograms and LC-MS spectra from an *in-vitro* reaction assay of different steroids (**A**, androstenedione; **B**, progesterone; and **C**, testosterone) with purified enzyme, CYP154C7. In each case, inset I (blue color) show the HPLC chromatograms of reaction mixtures, indicating peaks of products formed and substrates remaining. Insets II (black color) and III (red color) represent the standard peaks of substrates used and the targeted product, respectively. Whereas, insets IV and V contain LC-MS spectra of substrates and mono-hydroxylated products, respectively. The letter 'P' indicates the peak of the expected product.

of $C_{21}H_{31}O_3^+$ is 331.4698 amu (Fig. 2B and Table S3). For the steroid testosterone, the exact mass of the parent compound was m/z^+ $[M+H]^+$ 289.2167 amu, and the major product had an exact mass of m/z^+ $[M+H]^+$ 305.2103 amu. The calculated formula mass of $C_{19}H_{29}O_3^+$ is 305.4322 amu (Fig. 2C and Table S3). In each case, the observed exact masses of the steroid parent compounds and their respective mono-hydroxylated products closely match the theoretically calculated masses based on their chemical formula. These results suggest that the products formed from parent androstenedione, progesterone, and testosterone confirm the formation of the respective 16α-hydroxylated products.

The presence of functional groups such as hydroxyl, keto, alkyl, ester/ether, and carboxyl groups in steroids can significantly influence the hydroxylation pattern and selectivity [61,62]. A previous study reported that CYP154C5 and CYP154C8 exhibit higher selectivity for substrates with hydroxyl or keto groups at the C17 position compared to those with bulkier C17 substituents [43,63]. For CYP154C3_1 and CYP154C3_2 enzymes, the functional groups at the C11 and C21 positions have influenced hydroxylation patterns and product formation [46]. Similarly, CYP154C7 has been observed to exhibit comparable reaction patterns for steroids based on the functional groups. HPLC chromatograms of adrenosterone, cortisone, 11α-hydroxyprogesterone, prednisone, 17α-hydroxyprogesterone, and corticosterone reveal multiple peaks, indicating the influence of C17, C11, and C21 functional groups on product pattern formation (Fig. S5). Mass data analysis revealed that the major peaks in each substrate are mono-hydroxylated products. Prednisone and 17α-hydroxyprogesterone each produced two peaks (Figs. S5E–F), while corticosterone produced four peaks, with P1 being the major one (Fig. S5H). Nandrolone, in contrast, made a single peak (P) (Fig. S5G). Comparison with our previous results revealed that most major products involve 16α-position hydroxylation. Moreover, CYP154C8, CYP154C3_1, and CYP154C3_2 have been reported to produce 21α-hydroxycorticosterone from corticosterone, along with C-C bond cleavage products in cortisone and prednisone-like steroids [43,46]. Our HPLC chromatograms also suggest the possible production of 21α-hydroxycorticosterone and C-C bond

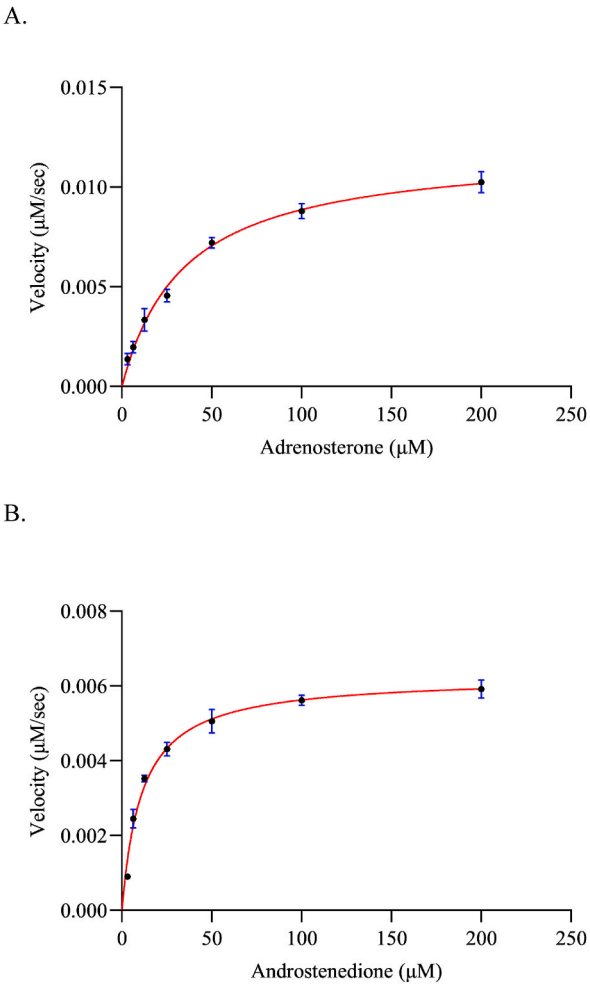

Fig. 3. Plots represent kinetic analysis using variable concentrations of adrenosterone (**A**) and androstenedione (**B**). The reaction mixture contained a ratio of CYP:Pdx:PdR at 1:8:2, with varying substrate concentrations. The reaction was initiated by the addition of 250 μM NADH, and the resulting rate of reaction was plotted against substrate concentration. The data were subjected to non-linear regression analysis based on Michaelis-Menten kinetics. Reported values represent the mean of three independent experiments under identical conditions, along with the standard deviation.

cleavage products. Overall, CYP154C7 has demonstrated a steroid conversion rate as effective as homologs (Fig. 1, Table S2).

3.4. Effect of temperature and pH on enzymatic activity and kinetic evaluation

The effects of incubation temperature and pH on the activity of CYP154C7 in the conversion of androstenedione were assessed as outlined in the Materials and Methods section. CYP154C7 displayed its highest hydroxylation activity at 30 °C (Fig. S6A), with a notable decline in activity at temperatures above 40 °C. Additionally, CYP154C7 showed pH stability within the 7.2–7.6 range, maintaining over 90 % of its maximal activity (Fig. S6B). These findings indicate that CYP154C7 operates most efficiently at 30 °C and pH 7.4, suggesting its suitability for optimal hydroxylation activity.

To augment our comprehension of the enzyme, we determined the kinetic parameters for purified CYP154C7, particularly focusing on the most converted steroids, such as androstenedione and adrenosterone. The K_m and V_{max} were calculated using heterologous redox partners Pdx and PdR from *P. putida*. CYP154C7 exhibited a greater affinity for androstenedione, as indicated by K_m and V_{max} values of (11.06 ± 1.903) μM and (0.0062 ± 0.0002) sec^{-1}, respectively. In contrast, adrenosterone displayed lower affinity, with a K_m value of (34.50 ± 6.2) μM and a V_{max} value of (0.0119 ± 0.0007) sec^{-1} (Fig. 3A–B).

3.5. Substrate-binding assay

Substrate binding to CYP enzymes induces a shift in ferric heme iron from a low-to high-spin state, observed as a change in the Soret absorption spectrum. This spin shift, resulting from the displacement of the heme-bound water ligand, is crucial to the CYP catalytic mechanism. The high-spin state is marked by a "type I shift," with a Soret absorption minimum of around 420 nm and a maximum of around 390 nm [63–65]. To investigate the potential occurrence of a type I spin shift in CYP154C7, we tested three steroids (androstenedione, testosterone, and cortisone) from our substrate list based on their different conversion rates. Upon binding to CYP154C7, these steroids indeed displayed a type I shift, characterized by an absorbance peak at 390 nm and a trough at 420 nm. The K_D values of substrates for CYP154C7 were determined by conducting titrations with different substrate concentrations until reaching saturation and then fitting the resulting data to a nonlinear tight-binding quadratic equation, as illustrated in figure (Fig. S7). The K_D values for androstenedione, and testosterone were determined to be less than 0.5 μM (0.2013 ± 0.043 and 0.3041 ± 0.070, respectively), indicating strong and tight binding. Notably, these substrates were among the most hydrophobic compounds used in the experiment. In contrast, the substrate cortisone exhibited a high K_D value (1.995 ± 0.340) and was assumed to be less hydrophobic than previous substrates. This suggests that reducing substrate hydrophobicity increases the K_D value, a finding consistent with reports on CYP154C3_1, CYP154C3_2, CYP154C5, and CYP154C8, which show tight binding with low K_D values to steroids. Hydrophobic interactions between steroids and the CYP active site increase activation entropy, enhancing catalytic efficiency. As hydrophobic steroids bind, low-entropy water molecules are displaced from both the active site and the steroid's solvation shell, significantly contributing to the total entropy change and facilitating hydrophobic contacts that improve binding and catalytic efficiency [66,67].

3.6. In-silico analysis

We performed homology modeling, molecular docking simulation, and substrate tunnel analysis to investigate protein structure

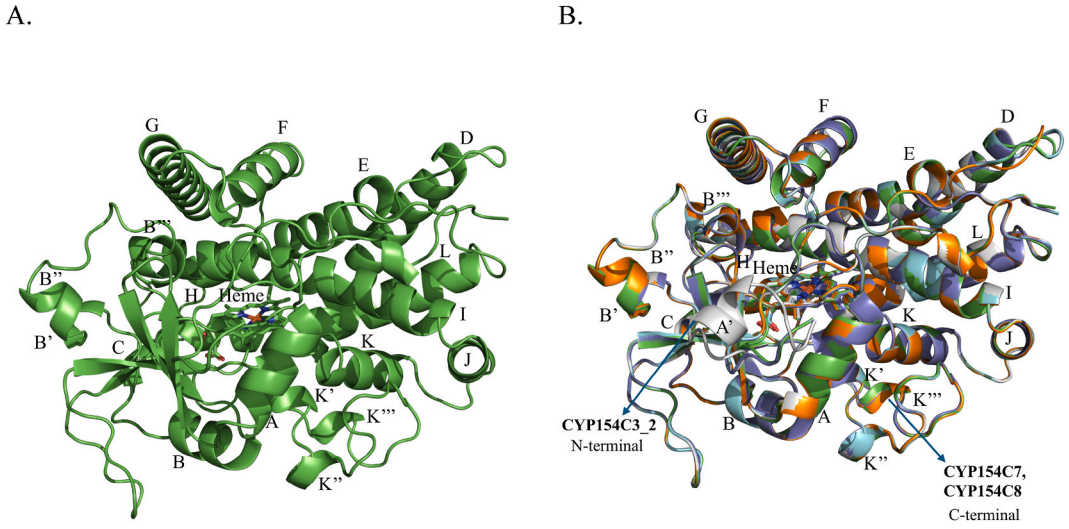

Fig. 4. Structures of selected CYPs for comparison are shown in ribbon models with P450 helix numbering, whereas heme is shown in stick representation. **A**. Homology model structure of CYP154C7. **B**. Overlay structure of CYP154C5 (PDB ID:6TO2) (violet) with the best homology models of CYP154C3_1 (cyan), CYP154C3_2 (white), CYP154C7 (green), and CYP154C8 (orange) indicating different in additional alpha-helices.

and function.

3.7. Homology modeling

The homology model of CYP154C7 and their homologs were generated and refined using the SWISS-MODEL, followed by validation through online programs. Online programs PROCHECK, ERRAT, and VERIFY-3D scores (data shown for only CYP154C7, Figs. S8A–C), affirmed the acceptability and trustworthiness of the optimized models. In comparison with the structure of CYP154C5 (*Nocardia farcinica*), the predicted structure of CYP154C7 (*Streptomyces* sp.), along with their homologs(*Streptomyces* sp.) (Fig. 4A–B), demonstrates numerous resemblances [66]. All proteins share a helix-dominant cytochrome P450 monooxygenase fold, characterized by a flattened hydrophobic substrate channel above the heme porphyrin. Within the internal cavity of the predicted homology models, various aromatic and aliphatic amino acids are aligned analogously to those in CYP154C5. Nonetheless, it has been observed that A85, Y197, K236, and T288 within the active site of CYP154C7 differ from CYP154C5, which features V87, F200, Q239, and V291, respectively. For CYP154C3_1, CYP154C3_2, and CYP154C8, all internal cavity amino acid positions are the same as in CYP154C7,

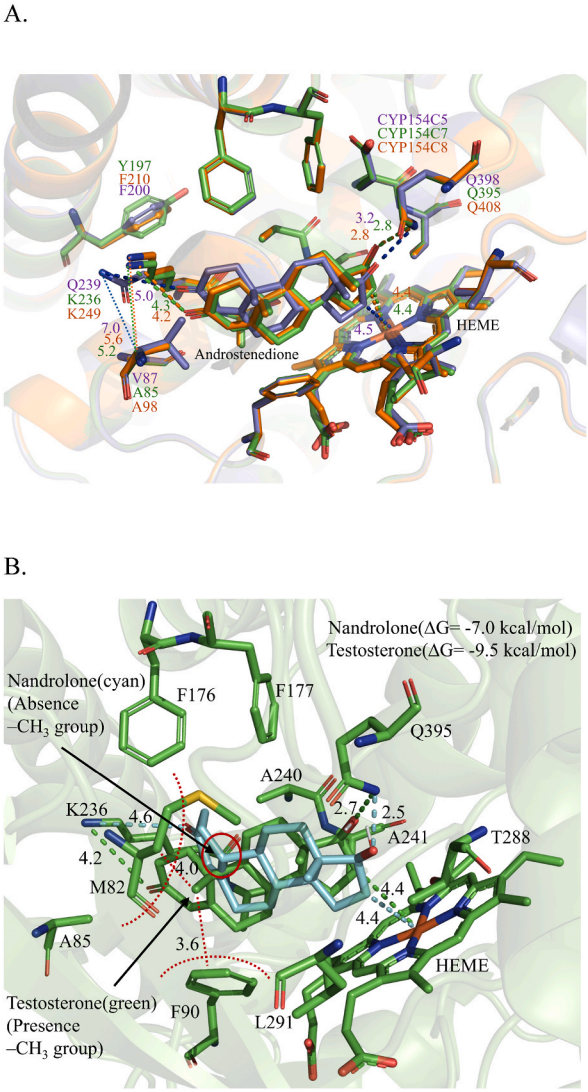

Fig. 5. A. Comparison of molecular docking analysis of CYPs (CYP154C5, violet; CYP154C7, green; and CYP154C8, orange) for androstenedione. Active site residues, heme, and androstenedione are shown in stick representation. The distance between heme (Fe) and the nearest carbon of androstenedione and the distance between steroids and key residues were measured. (Figure not shown for CYP154C3_1 and CYP154C3_2, a similar active site like CYP154C7). **B.** Testosterone and nandrolone binding modes in CYP154C7 along with respective (ΔG) values. Active site residues, heme, testosterone, and nandrolone are shown in stick representation. The distance between heme (Fe) and the nearest carbon of steroids and the distance between steroids and key residues were measured. Crucial residues (M82, F90) involved in hydrophobic interactions with the C10 positions of the steroids are shown with measured distances and a red-dotted semicircle.

except for F210 in CYP154C8, which corresponds to the analogous position in CYP154C5 (Fig. 5A). Furthermore, upon examining the superimposed figure of the predicted homology models with CYP154C5, we identified an additional sub-alpha helix present in the N-terminal of CYP154C3_2 (A'), and the C-terminal of both CYP154C8 and CYP154C7 (k'") (Fig. 4B).

3.8. Docking simulations

Using molecular docking, we examined the interaction of steroids with the active site of CYPs. Docked poses were selected based on the dominant ligand conformation and analyzed for binding modes with CYP. The binding energies for androstenedione, progesterone, and testosterone against CYP154C7 were determined to be −10.1, −8.0, and −9.5 kcal/mol, respectively, with distances between the Fe atom and C-16 measuring 4.4, 4.5, and 4.4 Å (Fig. 5A, S9, S10, and Table S4). These values indicate the suitability of these sites for 16α-hydroxylation, aligning with experimental HPLC and LC-MS data. Previous investigations have elucidated the crystal structure of CYP154C5, highlighting pivotal residues such as M84, F92, Q239, and Q398 involved in steroid binding. These residues are integral to the enzyme's regioselectivity and stereoselectivity during steroid hydroxylation [66]. Mutagenesis experiments have further demonstrated the importance of these residues, particularly showing that the Q239A mutant enhances steroid binding [68]. Since Q239 is replaced by lysine (K) in CYP154C3_1, CYP154C3_2, CYP154C7, and CYP154C8 while other critical residues remain conserved, lysine may influence hydroxylation conversion and substrate selectivity. Docking studies revealed a marginal impact on substrate binding compared to CYP154C5. Despite the lower binding energies observed in CYP154C3_1, CYP154C3_2, CYP154C7, and CYP154C8, the shorter distances between the substrates' C-16 and the heme, as well as between the C-17 functional group and key glutamine residues, and the O3 and lysine positions, indicate favorable conditions for steroid hydroxylation, resulting in better conversion as shown in Table S2. This suggests that lysine has also improved steroid accommodation in CYP154C3_1, CYP154C3_2, CYP154C7, and CYP154C8, resulting in stronger binding orientations with the heme and enhancing steroid oxidation, as confirmed by experimental data and previous studies.

Furthermore, CYP154C7 shows a distinct preference for specific substrates, notably favoring androstenedione (Table S4) and adrenosterone (docking data not shown), with a high conversion rate of over 95 % (Table S2). Steroids with a keto group at the C17 position have shown enhanced reactivity compared to others. However, Substituents at alternative positions are considered significant for substrate accommodation. For instance, testosterone, which has a higher conversion rate than nandrolone, contains a C-10 methyl group that nandrolone lacks. It is assumed that this absence in nandrolone exhibits weaker hydrophobic interactions with M82 and F90 (Fig. 5B), leading to reduced reactivity compared to testosterone. Previous studies indicate that enzymes CYP154C3_1, CYP154C3_2, and CYP154C8 preferentially interact with progesterone (Table S2). Progesterone positions itself near the heme group and key catalytic residues in these enzymes, facilitating the reaction (Fig. S9). Docking results of corticosterone in CYP154C7 reveal that binding energy ($\Delta G = -7.9$ kcal/mol) and orientation are likely influenced by the bulky C-17 group, with contributions from the C-11 functional group (Fig. S11). Similar orientations were observed for cortisone and prednisone (figure not shown), suggesting that the bulkier group at the C-17 position may effectively impact C-16 hydroxylation. These results highlight the crucial role of functional groups at the C-10, C-11, and C-17 positions in enhancing substrate selectivity for CYP154C7.

3.9. Substrate tunnel analysis

The substrate's accessibility and product exit efficiency significantly affect CYP enzyme catalytic activity. Therefore, we compared the substrate access channel in selected CYPs. CAVER analysis revealed that the substrate entry tunnel in CYP154C5 has a bottleneck near Q239 and V87, similar to the lysine and alanine residues in other CYPs (Fig. 6). The distances between Q239 and V87 (7 Å) in CYP154C5 and K249 and A98 (5.6 Å) in CYP154C8 are wider compared to other CYPs (5.2 Å) (Fig. 5A). Additionally, bottleneck radius

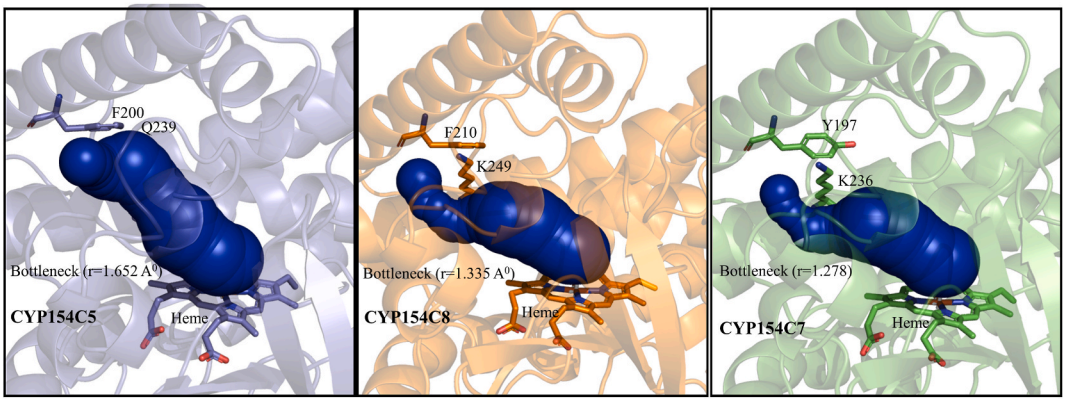

Fig. 6. Comparison of substrate access bottleneck in CYPs (CYP154C5, violet; CYP154C7, green; and CYP154C8, orange) as computed by CAVER 3.0, showing the key residues located at the side of the tunnel (blue color) were subjected to be responsible for facilitating substrate to the active site. (Figure not shown for CYP154C3_1 and CYP154C3_2, similar like CYP154C7).

of the substrate access tunnel follows the order CYP154C5 > CYP154C8 > C ≈ B ≈ A (Fig. 6), where a wider bottleneck facilitates substrate access and product egress, enhancing catalytic activity. Despite this, experimental results indicate that CYP154C7 is as effective as other CYPs in steroid hydroxylation, suggesting that nearby amino acids may influence substrate passage differently. We found that residue F200 in CYP154C5 and F210 in CYP154C8, as well as tyrosine (Y) at similar positions in other CYPs, may facilitate substrate entry into the tunnel by influencing the orientation of Q and K in their respective CYPs. We hypothesize that the hydroxyl group (-OH) on the tyrosine side chain may form additional hydrogen bonds, influencing the flexibility and dynamics of the access channel. This could enhance substrate accessibility and potentially increase catalytic efficiency. Recently, a study found that the M191F mutation in the access channel of CYP154C2 improved conversion efficiency and substrate selectivity, highlighting the impact of specific residues on catalytic performance [69]. Similarly, we propose that tyrosine (Y) present in CYP154C7, CYP154C3_1, and CYP154C3_2 has influenced substrate selectivity and catalytic efficiency, much like phenylalanine (F) in CYP154C8, CYP154C5, and the M191F mutant in CYP154C2.

3.10. Whole-cell biotransformation

Certain CYPs can utilize the inherent redox partners of *E. coli* for electron transfer during whole-cell bioconversion. However, CYP154C7 could not hydroxylate steroids with an *E. coli* redox partner, likely due to structural incompatibility with the endogenous partners in the BL21(DE3) strain [70,71]. While expressing Pdx and PdR may increase costs, it can improve biotransformation efficiency. Thus, *E. coli* BL21(DE3) cells were co-expressed with pET32a_CYP154C7 and a duet vector carrying Pdx and PdR (pCDFDuet) to facilitate the in-vivo bioconversion of externally added steroids. HPLC chromatograms of the extract from the biotransformation revealed peaks corresponding to the hydroxylated products of the respective substrates for five steroids. Androstenedione (97 %), progesterone (92 %), and adrenosterone (87 %) were converted significantly to hydroxylated products, while testosterone and nandrolone were converted around 53 % and 28 %, respectively (Fig. S12).

In addition, *in-vivo* biotransformation yielded a single mono-hydroxylated peak for some substrates. Steroids, androstenedione, progesterone, and testosterone have shown mono-hydroxylated peaks, hydroxylation occurred at 16α-position of the steroid ring, confirmed by co-elution with standard substrates and mass data results analysis (Figs. S13A–C). The other two steroids, adrenosterone, and nandrolone have shown mono-hydroxylated single peaks supporting the possible 16α-hydroxylated product formation (Figs. S13D–E). This result indicates the promising potential of CYP154C7 for future rational design and application as a whole-cell biocatalyst to produce derivatives of hydroxylated steroid compounds.

4. Conclusions

In summary, our investigation focused on the function and structure of CYP154C7 isolated from *Streptomyces* sp. PAMC26508, aiming to characterize its hydroxylating activity and analyze its structure for insights into steroid hydroxylases. Based on the results, CYP154C7 can be a potential candidate for producing hydroxylated steroids for various biological applications. Furthermore, the homology model and docking results reveal that CYP154C7, as well as CYP154C8, CYP154C3_1, and CYP154C3_2, utilize a highly similar set of residues for binding steroids, akin to related steroid hydroxylases such as CYP154C5. Comparative docking studies highlight the key residue lysine (K), similarly positioned to Q239 in CYP154C5, which influences steroid binding favorably. Additionally, it has been considered the access channel residue tyrosine (Y) in CYP154C7, CYP154C3_1, and CYP154C3_2 similar in position to residue 200F in CYP154C5 and residue 210F in CYP154C8, could facilitate substrate entry into the tunnel and increase in catalytic efficiency. Overall, these results provide useful insights for subsequent protein engineering of CYP steroid hydroxylases to enable the production of modified steroid compounds with more potent bioactivities.

CRediT authorship contribution statement

Prakash Paudel: Writing – review & editing, Writing – original draft, Methodology, Investigation, Formal analysis, Data curation, Conceptualization. **Kamal Prasad Regmi:** Writing – review & editing, Writing – original draft, Methodology, Investigation, Formal analysis, Data curation, Conceptualization. **Ki-Hwa Kim:** Writing – review & editing, Writing – original draft, Methodology, Investigation. **Jun Hyuck Lee:** Writing – review & editing, Writing – original draft. **Tae-Jin Oh:** Writing – review & editing, Writing – original draft, Supervision, Resources, Project administration, Investigation, Funding acquisition, Conceptualization.

Data availability statement

All relevant data are included in the main manuscript and the supplementary materials.

Funding

This work was supported by the project titled “Development of potential antibiotic compounds using polar organism resources (20200610)”, funded by the Ministry of Oceans and Fisheries, Korea.

Declaration of competing interest

The authors declare that they have no known competing financial interests or personal relationships that could have appeared to influence the work reported in this paper.

Appendix ASupplementary data

Supplementary data to this article can be found online at https://doi.org/10.1016/j.heliyon.2024.e39777.

References

[1] W.L. Miller, R.J. Auchus, The molecular biology, biochemistry, and physiology of human steroidogenesis and its disorders, Endocr. Rev. 32 (2011) 81–151, https://doi.org/10.1210/er.2010-0013.

[2] N. Sultana, Microbial biotransformation of bioactive and clinically useful steroids and some salient features of steroids and biotransformation, Steroids 136 (2018) 76–92, https://doi.org/10.1016/j.steroids.2018.01.007.

[3] S. Ke, Recent progress of novel steroid derivatives and their potential biological properties, Mini-Rev. Med. Chem. 18 (2018) 745–775, https://doi.org/10.2174/1389557517666171003103245.

[4] J.A.R. Salvador, J.F.S. Carvalho, M.A.C. Neves, S.M. Silvestre, A.J. Leitão, M.M.C. Silva, M.L. Sá e Melo, Anticancer steroids: linking natural and semi-synthetic compounds, Nat. Prod. Rep. 30 (2013) 324–374, https://doi.org/10.1039/C2NP20082A.

[5] V.M. Dembitsky, Antitumor and hepatoprotective activity of natural and synthetic neo steroids, Prog. Lipid Res. 79 (2020) 101048, https://doi.org/10.1016/j.plipres.2020.101048.

[6] S.C. Manolagas, Steroids and osteoporosis: the quest for mechanisms, J. Clin. Invest. 123 (2013) 1919–1921, https://doi.org/10.1172/JCI68062.

[7] J.T. Price, B. Vwalika, B.L. Freeman, S.R. Cole, P.T. Saha, F.M. Mbewe, W.M. Phiri, M. Peterson, D. Muyangwa, N. Sindano, H. Mwape, M.E. Smithmyer, M. P. Kasaro, D.J. Rouse, R.L. Goldenberg, E. Chomba, J.S.A. Stringer, Weekly 17 alpha-hydroxyprogesterone caproate to prevent preterm birth among women living with HIV: a randomised, double-blind, placebo-controlled trial, Lancet HIV 8 (2021) e605–e613, https://doi.org/10.1016/S2352-3018(21)00150-8.

[8] G.W. Waterer, J. Rello, Steroids and COVID-19: we need a precision approach, not one size fits all, Infect. Dis. Ther. 9 (2020) 701–705, https://doi.org/10.1007/s40121-020-00338-x.

[9] B. Ruiz-Antorán, A. Sancho-López, F. Torres, V. Moreno-Torres, I. de Pablo-López, P. García-López, F. Abad-Santos, C.M. Rosso-Fernández, A. Aldea-Perona, E. Montané, R.M. Aparicio-Hernández, R. Llop-Rius, C. Pedrós, P. Gijón, C. Hernández-Carballo, M.J. Pedrosa-Martínez, C. Rodríguez-Jiménez, G. Prada-Ramallal, L. Cabrera-García, J.A. Aguilar-García, R. Sanjuan-Jimenez, E.I. Ortiz-Barraza, E. Sánchez-Chica, A. Fernández-Cruz, Combination of tocilizumab and steroids to improve mortality in patients with severe COVID-19 infection: a Spanish, multicenter, cohort study, Infect. Dis. Ther. 10 (2021) 347–362, https://doi.org/10.1007/s40121-020-00373-8.

[10] A.G. Fragkaki, Y.S. Angelis, M. Koupparis, A. Tsantili-Kakoulidou, G. Kokotos, C. Georgakopoulos, Structural characteristics of anabolic androgenic steroids contributing to binding to the androgen receptor and to their anabolic and androgenic activities, Steroids 74 (2009) 172–197, https://doi.org/10.1016/j.steroids.2008.10.016.

[11] D. Lembo, V. Cagno, A. Civra, G. Poli, Oxysterols: an emerging class of broad spectrum antiviral effectors, Mol. Aspect. Med. 49 (2016) 23–30, https://doi.org/10.1016/j.mam.2016.04.003.

[12] J. Nikolaus, K.T. Nguyen, C. Virus, J.L. Riehm, M. Hutter, R. Bernhardt, Engineering of CYP106A2 for steroid 9α- and 6β-hydroxylation, Steroids 120 (2017) 41–48, https://doi.org/10.1016/j.steroids.2017.01.005.

[13] A. Van der Willigen, J.D. Peereboom-Wynia, T. Van Joost, E. Stolz, A preliminary study of the effect of 11a-hydroxyprogesterone on the hair growth in men suffering from androgenetic alopecia, Acta Derm. Venereol. 67 (1987) 82–85, https://doi.org/10.2340/00015555678285.

[14] N. Milecka-Tronina, T. Kołek, A. Świzdor, A. Panek, Hydroxylation of DHEA and its analogues by Absidia coerulea AM93. Can an inducible microbial hydroxylase catalyze 7α- and 7β-hydroxylation of 5-ene and 5α-dihydro C19-steroids? Bioorg. Med. Chem. 22 (2014) 883–891, https://doi.org/10.1016/j.bmc.2013.11.050.

[15] K. Wojtal, M.K. Trojnar, S.J. Czuczwar, Endogenous neuroprotective factors: neurosteroids, Pharmacol. Rep. 58 (2006) 335–340. http://www.ncbi.nlm.nih.gov/pubmed/16845207.

[16] S.A. Ali Shah, S. Sultan, H.S. Adnan, A whole-cell biocatalysis application of steroidal drugs, Orient. J. Chem. 29 (2013) 389–403, https://doi.org/10.13005/ojc/290201.

[17] J.R. Berrie, R.A.D. Williams, K.E. Smith, Microbial transformations of steroids-XI. Progesterone transformation by Streptomyces roseochromogenes–purification and characterisation of the 16α-hydroxylase system, J. Steroid Biochem. Mol. Biol. 71 (1999) 153–165, https://doi.org/10.1016/S0960-0760(99)00132-6.

[18] F.Z. Stanczyk, D.F. Archer, Gestodene: a review of its pharmacology, potency and tolerability in combined contraceptive preparations, Contraception 89 (2014) 242–252, https://doi.org/10.1016/j.contraception.2013.12.003.

[19] T.G. Lobastova, S.A. Gulevskaya, G.V. Sukhodolskaya, M.V. Donova, Dihydroxylation of dehydroepiandrosterone in positions 7α and 15α by mycelial fungi, Appl. Biochem. Microbiol. 45 (2009) 617–622, https://doi.org/10.1134/S0003683809060076.

[20] X. Zhang, Y. Peng, J. Zhao, Q. Li, X. Yu, C.G. Acevedo-Rocha, A. Li, Bacterial cytochrome P450-catalyzed regio- and stereoselective steroid hydroxylation enabled by directed evolution and rational design, Bioresour. Bioprocess. 7 (2020) 2, https://doi.org/10.1186/s40643-019-0290-4.

[21] H. Ichinose, Molecular and functional diversity of fungal cytochrome P450s, Biol. Pharm. Bull. 35 (2012) 833–837, https://doi.org/10.1248/bpb.35.833.

[22] D.C. Lamb, L. Lei, A.G.S. Warrilow, G.I. Lepesheva, J.G.L. Mullins, M.R. Waterman, S.L. Kelly, The first virally encoded cytochrome P450, J. Virol. 83 (2009) 8266–8269, https://doi.org/10.1128/JVI.00289-09.

[23] D.R. Nelson, Cytochrome P450 diversity in the tree of life, Biochim. Biophys. Acta, Proteins Proteomics 1866 (2018) 141–154, https://doi.org/10.1016/j.bbapap.2017.05.003.

[24] R. Bernhardt, Cytochromes P450 as versatile biocatalysts, J. Biotechnol. 124 (2006) 128–145, https://doi.org/10.1016/j.jbiotec.2006.01.026.

[25] D. Schmitz, S. Janocha, F.M. Kiss, R. Bernhardt, CYP106A2—a versatile biocatalyst with high potential for biotechnological production of selectively hydroxylated steroid and terpenoid compounds, Biochim. Biophys. Acta, Proteins Proteomics 1866 (2018) 11–22, https://doi.org/10.1016/j.bbapap.2017.07.011.

[26] K.S. Halskov, B.S. Donslund, S. Barfüsser, K.A. Jørgensen, Organocatalytic asymmetric formation of steroids, Angew. Chem. Int. Ed. 53 (2014) 4137–4141, https://doi.org/10.1002/anie.201400203.

[27] M. Bureik, R. Bernhardt, Steroid hydroxylation: microbial steroid biotransformations using cytochrome P450 enzymes, in: Mod. Biooxidation, Wiley, 2007, pp. 155–176, https://doi.org/10.1002/9783527611522.ch6.

[28] I. Kaluzna, T. Schmitges, H. Straatman, D. van Tegelen, M. Müller, M. Schürmann, D. Mink, Enabling selective and sustainable P450 oxygenation technology. Production of 4-Hydroxy-α-isophorone on kilogram scale, Org. Process Res. Dev. 20 (2016) 814–819, https://doi.org/10.1021/acs.oprd.5b00282.

[29] C.J.C. Whitehouse, S.G. Bell, L. Wong, ChemInform abstract: P450 BM3 (CYP102A1): connecting the dots, ChemInform 43 (2012), https://doi.org/10.1002/chin.201217268.

[30] A. Li, C.G. Acevedo-Rocha, L. D'Amore, J. Chen, Y. Peng, M. Garcia-Borràs, C. Gao, J. Zhu, H. Rickerby, S. Osuna, J. Zhou, M.T. Reetz, Regio- and stereoselective steroid hydroxylation at C7 by cytochrome P450 monooxygenase mutants, Angew. Chem. Int. Ed. 59 (2020) 12499–12505, https://doi.org/10.1002/anie.202003139.

[31] B.D. Pardhe, K.P. Kwon, J.K. Park, J.H. Lee, T.-J. Oh, H 2 O 2 -driven hydroxylation of steroids catalyzed by cytochrome P450 CYP105D18: exploration of the substrate access channel, Appl. Environ. Microbiol. 89 (2023), https://doi.org/10.1128/aem.01585-22.

[32] B. Ma, Q. Wang, H. Ikeda, C. Zhang, L.-H. Xu, Hydroxylation of steroids by a microbial substrate-promiscuous P450 cytochrome (CYP105D7): key arginine residues for rational design, Appl. Environ. Microbiol. 85 (2019), https://doi.org/10.1128/AEM.01530-19.

[33] H. Agematu, N. Matsumoto, Y. Fujii, H. Kabumoto, S. Doi, K. Machida, J. Ishikawa, A. Arisawa, Hydroxylation of testosterone by bacterial cytochromes P450 using the Escherichia coli expression system, Biosci. Biotechnol. Biochem. 70 (2006) 307–311, https://doi.org/10.1271/bbb.70.307.

[34] F.M. Kiss, D. Schmitz, J. Zapp, T.K.F. Dier, D.A. Volmer, R. Bernhardt, Comparison of CYP106A1 and CYP106A2 from Bacillus megaterium – identification of a novel 11-oxidase activity, Appl. Microbiol. Biotechnol. 99 (2015) 8495–8514, https://doi.org/10.1007/s00253-015-6563-8.

[35] K.-H. Kim, H. Do, C.W. Lee, P. Subedi, M. Choi, Y. Nam, J.H. Lee, T.-J. Oh, Crystal structure and biochemical analysis of a cytochrome P450 steroid hydroxylase (Ba CYP106A6) from Bacillus species, J. Microbiol. Biotechnol. 33 (2023) 387–397, https://doi.org/10.4014/jmb.2211.11031.

[36] X. Zhang, Y. Hu, W. Peng, C. Gao, Q. Xing, B. Wang, A. Li, Exploring the potential of cytochrome P450 CYP109B1 catalyzed regio—and stereoselective steroid hydroxylation, Front. Chem. 9 (2021), https://doi.org/10.3389/fchem.2021.649000.

[37] I.K. Jóźwik, F.M. Kiss, Ł. Gricman, A. Abdulmughni, E. Brill, J. Zapp, J. Pleiss, R. Bernhardt, A.W.H. Thunnissen, Structural basis of steroid binding and oxidation by the cytochrome P450 <scp>CYP</scp> 109E1 from *Bacillus megaterium*, FEBS J. 283 (2016) 4128–4148, https://doi.org/10.1111/febs.13911.

[38] I.K. Jóźwik, E. Bombino, A. Abdulmughni, P. Hartz, H.J. Rozeboom, H.J. Wijma, R. Kappl, D.B. Janssen, R. Bernhardt, A.W.H. Thunnissen, Regio- and stereoselective steroid hydroxylation by <scp>CYP109A2</scp> from *Bacillus megaterium* explored by X-ray crystallography and computational modeling, FEBS J. 290 (2023) 5016–5035, https://doi.org/10.1111/febs.16906.

[39] J.M. Klenk, P. Dubiel, M. Sharma, G. Grogan, B. Hauer, Characterization and structure-guided engineering of the novel versatile terpene monooxygenase <scp>CYP</scp> 109Q5 from *Chondromyces apiculatus* <scp>DSM</scp> 436, Microb. Biotechnol. 12 (2019) 377–391, https://doi.org/10.1111/1751-7915.13354.

[40] Y. Khatri, Y. Carius, M. Ringle, C.R.D. Lancaster, R. Bernhardt, Structural characterization of <scp>CYP</scp> 260A1 from *Sorangium cellulosum* to investigate the 1α-hydroxylation of a mineralocorticoid, FEBS Lett. 590 (2016) 4638–4648, https://doi.org/10.1002/1873-3468.12479.

[41] S.G. Salamanca-Pinzon, Y. Khatri, Y. Carius, L. Keller, R. Müller, C.R.D. Lancaster, R. Bernhardt, Structure–function analysis for the hydroxylation of Δ4 C21-steroids by the myxobacterial CYP260B1, FEBS Lett. 590 (2016) 1838–1851, https://doi.org/10.1002/1873-3468.12217.

[42] Q. Wang, B. Ma, S. Fushinobu, C. Zhang, L.-H. Xu, Regio- and stereoselective hydroxylation of testosterone by a novel cytochrome P450 154C2 from Streptomyces avermitilis, Biochem. Biophys. Res. Commun. 522 (2020) 355–361, https://doi.org/10.1016/j.bbrc.2019.11.091.

[43] B. Dangi, K. Kim, S. Kang, T. Oh, Tracking down a new steroid-hydroxylating promiscuous cytochrome P450: CYP154C8 from Streptomyces sp. W2233-SM, Chembiochem 19 (2018) 1066–1077, https://doi.org/10.1002/cbic.201800018.

[44] B. Dangi, C.W. Lee, K. Kim, S. Park, E. Yu, C. Jeong, H. Park, J.H. Lee, T. Oh, Characterization of two steroid hydroxylases from different Streptomyces spp. and their ligand-bound and -unbound crystal structures, FEBS J. 286 (2019) 1683–1699, https://doi.org/10.1111/febs.14729.

[45] T. Makino, Y. Katsuyama, T. Otomatsu, N. Misawa, Y. Ohnishi, Regio- and stereospecific hydroxylation of various steroids at the 16α position of the D ring by the Streptomyces griseus cytochrome P450 CYP154C3, Appl. Environ. Microbiol. 80 (2014) 1371–1379, https://doi.org/10.1128/AEM.03504-13.

[46] P. Subedi, K.-H. Kim, Y.-S. Hong, J.-H. Lee, T.-J. Oh, Enzymatic characterization and comparison of two steroid hydroxylases CYP154C3-1 and CYP154C3-2 from Streptomyces species, J. Microbiol. Biotechnol. 31 (2021) 464–474, https://doi.org/10.4014/jmb.2010.10020.

[47] F. Madeira, M. Pearce, A.R.N. Tivey, P. Basutkar, J. Lee, O. Edbali, N. Madhusoodanan, A. Kolesnikov, R. Lopez, Search and sequence analysis tools services from EMBL-EBI in 2022, Nucleic Acids Res. 50 (2022) W276–W279, https://doi.org/10.1093/nar/gkac240.

[48] P. Gouet, E. Courcelle, D.I. Stuart, F. M√©toz, ESPript: analysis of multiple sequence alignments in PostScript, Bioinformatics 15 (1999) 305–308, https://doi.org/10.1093/bioinformatics/15.4.305.

[49] S. Kumar, G. Stecher, M. Li, C. Knyaz, K. Tamura, Mega X: molecular evolutionary genetics analysis across computing platforms, Mol. Biol. Evol. 35 (2018) 1547–1549, https://doi.org/10.1093/molbev/msy096.

[50] E. Zuckerkandl, L. Pauling, Evolutionary divergence and convergence in proteins, in: Evol. Genes Proteins, Elsevier, 1965, pp. 97–166, https://doi.org/10.1016/B978-1-4832-2734-4.50017-6.

[51] S. Bhattarai, K. Liou, T.-J. Oh, Hydroxylation of long chain fatty acids by CYP147F1, a new cytochrome P450 subfamily protein from Streptomyces peucetius, Arch. Biochem. Biophys. 539 (2013) 63–69, https://doi.org/10.1016/j.abb.2013.09.008.

[52] J.W. Williams, J.F. Morrison, [17] the kinetics of reversible tight-binding inhibition, 437–467. https://doi.org/10.1016/0076-6879(79)63019-7, 1979.

[53] R.A. Laskowski, M.W. MacArthur, D.S. Moss, J.M. Thornton, PROCHECK: a program to check the stereochemical quality of protein structures, J. Appl. Crystallogr. 26 (1993) 283–291, https://doi.org/10.1107/S0021889892009944.

[54] D. Eisenberg, R. Lüthy, J.U. Bowie, [20] VERIFY3D: assessment of protein models with three-dimensional profiles, 396–404, https://doi.org/10.1016/S0076-6879(97)77022-8, 1997.

[55] J.U. Bowie, R. Lüthy, D. Eisenberg, A method to identify protein sequences that fold into a known three-dimensional structure, Science 253 (1991) 164–170, https://doi.org/10.1126/science.1853201.

[56] O. Trott, A.J. Olson, AutoDock Vina: improving the speed and accuracy of docking with a new scoring function, efficient optimization, and multithreading, J. Comput. Chem. 31 (2010) 455–461, https://doi.org/10.1002/jcc.21334.

[57] G.M. Morris, R. Huey, W. Lindstrom, M.F. Sanner, R.K. Belew, D.S. Goodsell, A.J. Olson, AutoDock4 and AutoDockTools4: automated docking with selective receptor flexibility, J. Comput. Chem. 30 (2009) 2785–2791, https://doi.org/10.1002/jcc.21256.

[58] P. Warren L. DeLano, W.L. DeLano, PyMOL: an open-source molecular graphics tool, CCP4 Newsl Protein Crystallogr 40 (2002) 82–92 (n.d.), http://legacy.ccp4.ac.uk/newsletters/%0Anewsletter40.

[59] E. Chovancova, A. Pavelka, P. Benes, O. Strnad, J. Brezovsky, B. Kozlikova, A. Gora, V. Sustr, M. Klvana, P. Medek, L. Biedermannova, J. Sochor, J. Damborsky, Caver 3.0: a tool for the analysis of transport pathways in dynamic protein structures, PLoS Comput. Biol. 8 (2012) e1002708, https://doi.org/10.1371/journal.pcbi.1002708.

[60] B. Dangi, H. Park, T. Oh, Effects of alternative redox partners and oxidizing agents on CYP154C8 catalytic activity and product distribution, Chembiochem 19 (2018) 2273–2282, https://doi.org/10.1002/cbic.201800284.

[61] E.R.H. Jones, The microbiological hydroxylation of steroids and related compounds, Pure Appl. Chem. 33 (1973) 39–52, https://doi.org/10.1351/pac197333010039.

[62] R. Sen, T.B. Samanta, Influence of the substituents at C11 on hydroxylation at C6, of C21-steroids by Syncephalastrum racemosum, J. Steroid Biochem. 14 (1981) 307–309, https://doi.org/10.1016/0022-4731(81)90141-2.

[63] E.M. Isin, F.P. Guengerich, Substrate binding to cytochromes P450, Anal. Bioanal. Chem. 392 (2008) 1019–1030, https://doi.org/10.1007/s00216-008-2244-0.

[64] C. Jung, O. Ristau, H. Rein, The high-spin/low-spin equilibrium in cytochrome P-450 — a new method for determination of the high-spin content, Biochim. Biophys. Acta Protein Struct. Mol. Enzymol. 1076 (1991) 130–136, https://doi.org/10.1016/0167-4838(91)90229-S.

[65] I.G. Denisov, T.M. Makris, S.G. Sligar, I. Schlichting, Structure and chemistry of cytochrome P450, Chem. Rev. 105 (2005) 2253–2278, https://doi.org/10.1021/cr0307143.

[66] K. Herzog, P. Bracco, A. Onoda, T. Hayashi, K. Hoffmann, A. Schallmey, Enzyme–substrate complex structures of CYP154C5 shed light on its mode of highly selective steroid hydroxylation, Acta Crystallogr. Sect. D Biol. Crystallogr. 70 (2014) 2875–2889, https://doi.org/10.1107/S1399004714019129.

[67] P. Cozzini, M. Fornabaio, A. Marabotti, D.J. Abraham, G.E. Kellogg, A. Mozzarelli, Free energy of ligand binding to protein: evaluation of the contribution of water molecules by computational methods, Curr. Med. Chem. 11 (2004) 3093–3118, https://doi.org/10.2174/0929867043363929.

[68] P. Bracco, H.J. Wijma, B. Nicolai, J.A.R. Buitrago, T. Klünemann, A. Vila, P. Schrepfer, W. Blankenfeldt, D.B. Janssen, A. Schallmey, CYP154C5 regioselectivity in steroid hydroxylation explored by substrate modifications and protein engineering, Chembiochem 22 (2021) 1099–1110, https://doi.org/10.1002/cbic.202000735.

[69] Q. Gao, B. Ma, Q. Wang, H. Zhang, S. Fushinobu, J. Yang, S. Lin, K. Sun, B.-N. Han, L.-H. Xu, Improved 2α-hydroxylation efficiency of steroids by CYP154C2 using structure-guided rational design, Appl. Environ. Microbiol. 89 (2023), https://doi.org/10.1128/aem.02186-22.

[70] W. Zhang, L. Du, F. Li, X. Zhang, Z. Qu, L. Han, Z. Li, J. Sun, F. Qi, Q. Yao, Y. Sun, C. Geng, S. Li, Mechanistic insights into interactions between bacterial class I P450 enzymes and redox partners, ACS Catal. 8 (2018) 9992–10003, https://doi.org/10.1021/acscatal.8b02913.

[71] P.J. Bakkes, J.L. Riehm, T. Sagadin, A. Rühlmann, P. Schubert, S. Biemann, M. Girhard, M.C. Hutter, R. Bernhardt, V.B. Urlacher, Engineering of versatile redox partner fusions that support monooxygenase activity of functionally diverse cytochrome P450s, Sci. Rep. 7 (2017) 9570, https://doi.org/10.1038/s41598-017-10075-w.